



Short communication

Raman and infrared spectroscopy of Ge nanoparticles embedded in ZnO matrix

U. Pal*, J. García Serrano

Instituto de Física, Universidad Autónoma de Puebla, Apdo. Postal J-48, Puebla, Pue. 72570, Mexico

Received 14 July 2004; accepted 12 November 2004
Available online 19 December 2004

Abstract

Ge nanoparticles of 2.3–5.0 nm size embedded in ZnO matrix were prepared by rf alternate sputtering and subsequent annealing technique. Raman and infrared (IR) absorption spectroscopy were used to characterize the Ge/ZnO nanocomposite films. Raman spectra of the composite films revealed 300 cm^{-1} Ge–Ge transverse optic (TO) vibrational band of Ge nanocrystals, which shifted towards lower frequencies on decreasing the size of Ge nanocrystals due to phonon confinement in smaller crystallites. IR spectra of the composite films revealed that the Ge nanocrystals remain with elemental core surrounded by oxidized cap-layer. The thickness of the oxide cap-layer decreased with the increase of annealing temperature. © 2004 Elsevier B.V. All rights reserved.

PACS: 78.30.Am; 78.55.Ap; 78.66.Sq; 78.67.Bf

Keywords: Nanocomposites; Semiconductors; Raman spectroscopy; Infrared spectroscopy

1. Introduction

In recent years, the optical properties of semiconductor nanoparticles embedded in glass matrices have received considerable attention due to their potential applications in chemical catalysis [1,2], electronic and optical devices [3,4]. Semiconductor nanoparticles exhibit new quantum phenomena due to an increase in band gap with decreasing dimension

and discrete electronic states with higher oscillator strength. Surface electronic states in such quantum dots affect strongly their optical and electronic properties [4–6]. Though, the nanoparticles of several semiconductors like CdS and CdSe have been studied extensively, the recent revelations of strong photoluminescence (PL) emission from semiconductors nanoparticles of indirect band gap like Si and Ge have generated much interest in these materials [7–10]. In fact, very recently our group [11] and Hayashi et al. [12] have reported an indirect-to-direct band gap transition in small Ge nanoparticles. Though, Si and Ge nanocrystals (nc-Ge) have received widespread

* Corresponding author. Tel.: +52 222 229500;
fax: +52 222 2295611.

E-mail address: upal@sirio.ifuap.buap.mx (U. Pal).

research interest due to their good compatibility with conventional silicon-based integrated-circuit technology and high room temperature PL [5,13–15], due to its larger dielectric constant and smaller effective masses of electrons and holes in comparison to Si, it is easier to manipulate the electronic structure of Ge around its band gap.

Several works have been reported on the synthesis of Ge nanocrystals either as colloidal particle [16] or incorporated in SiO₂ matrix using several techniques [17–22] and their optical characterizations [19,20,23,24]. However, there are very few reports [11] on the synthesis of Ge nanocrystals and their optical properties in ZnO matrix. Being an electrode material, incorporation of nc-Ge in ZnO might be interesting to tailor its electronic properties suitable for electrolysis and catalytic applications.

We prepared Ge nanocrystals embedded in ZnO matrix by radio frequency alternate sputtering technique and annealed subsequently at different temperatures in Ar. The samples were characterized by transmission electron microscopy (TEM), Raman and infrared spectroscopy at room temperature. Effects of thermal annealing on the size of the nanoparticles and their behavior in Raman and IR spectra have been studied.

2. Experiment

Ge/ZnO composite films were prepared on quartz glass substrates by alternate deposition of ZnO and Ge using an rf magnetron sputtering system. At 45 mTorr argon partial pressure, the films of ZnO and Ge were deposited on quartz glass substrates alternatively using a 100 W rf power. A ZnO film of about 80 nm was first deposited on the quartz glass by sputtering a ZnO target (5 cm diameter, 99.995%) for 10 min and then a Ge film of about 6 nm was deposited by sputtering a Ge target (5 cm diameter, 99.999%) for 1 min. The process was repeated for six times, and depositing a ZnO layer at last, the deposition process was terminated. The whole process was carried out by changing the substrate position on different targets (i.e. on ZnO and Ge targets), i.e. without bringing the films outside the deposition chamber before completing the deposition process. The total thickness of the structure was about 600 nm. For the transmission

electron microscopic (TEM) observations, the samples were prepared as follows: A 20 nm layer of ZnO was first deposited on a carbon coated NaCl pallet; then a layer of Ge of about 6 nm thickness was grown on it, and another 20 nm ZnO layer was grown on the Ge layer. The as-grown samples were annealed at 200, 400 and 600 °C for 15 min in argon atmosphere.

A JEOL, JEM2000-FXII electron microscope was used for TEM observation on the samples. Raman spectra were obtained on a Dilor Lambram micro-Raman spectrometer at room temperature. The 632.8 nm line from a He–Ne laser was used as the excitation source. A Nicolet Magna 750 FTIR spectrometer was used to record the IR absorption spectra in diffuse mode.

3. Results and discussion

Fig. 1 shows the TEM micrographs of Ge/ZnO nanocomposites annealed at different temperatures. Formation of nanoparticles is clear from the micrographs. Depending on the temperature of annealing, nanoparticles of different average size were formed in the matrix. The values of average size of the nanoparticles in the composite samples annealed at different temperatures are given in Table 1.

Fig. 2 shows the Raman spectrum of a ZnO film without heat treatment. The spectrum revealed six peaks located at around 99, 445, 586, 817, 1372 and 1593 cm⁻¹. The peaks at about 99 and 445 cm⁻¹ were assigned to the two nonpolar Raman active E_2 vibrational modes of ZnO. The first peak is associated to the $E_2^{(1)}$ mode and its frequency is consistent with reported values for thin film and bulk ZnO samples [25]. While, the second peak is due to the $E_2^{(2)}$ mode characteristic of the wurtzite phase of the ZnO [25–27]. The peak at around 586 cm⁻¹ was assigned to

Table 1
Temperature variation of particle size of Ge and ZnO in Ge/ZnO composite films

Annealing temperature (°C)	Particle size of Ge (nm)	Particle size of ZnO (nm)
RT (as-deposited)	5.0	9.0
200	4.4	13.5
400	2.5	14.0
600	2.3	17.0

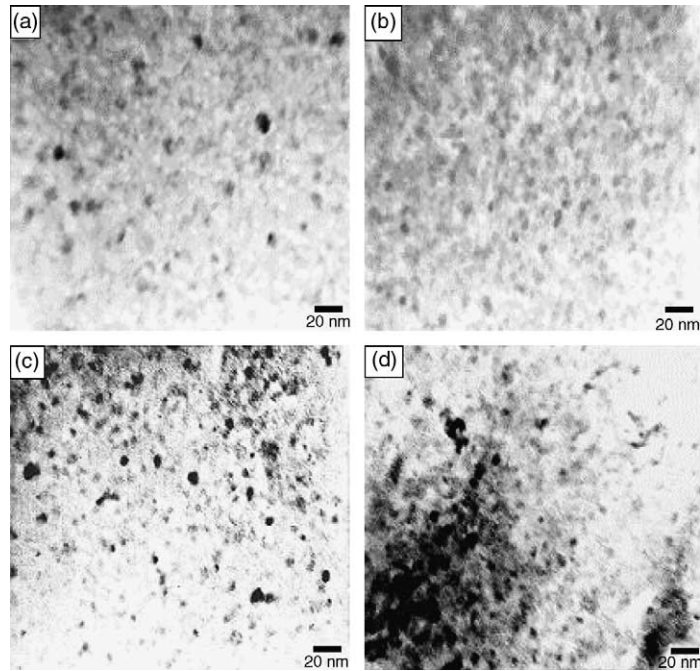


Fig. 1. TEM micrographs of Ge/ZnO composite films: (a) unannealed, (b) annealed at 200 °C, (c) annealed at 400 °C and (d) annealed at 600 °C.

the $E_1(\text{LO})$ mode of the ZnO [23]. The remaining peaks have not been assigned to any phonon mode, and probably correspond to the nanosized ZnO particles in the films. Recently, Zhou et al. [28] have reported the

existence of Raman peaks around 750, 850, 950 and 1050 cm^{-1} in nanoparticle or quantum dots of ZnO.

In Fig. 3, the Raman spectra for the ZnO and Ge/ZnO composite films annealed at different tempera-

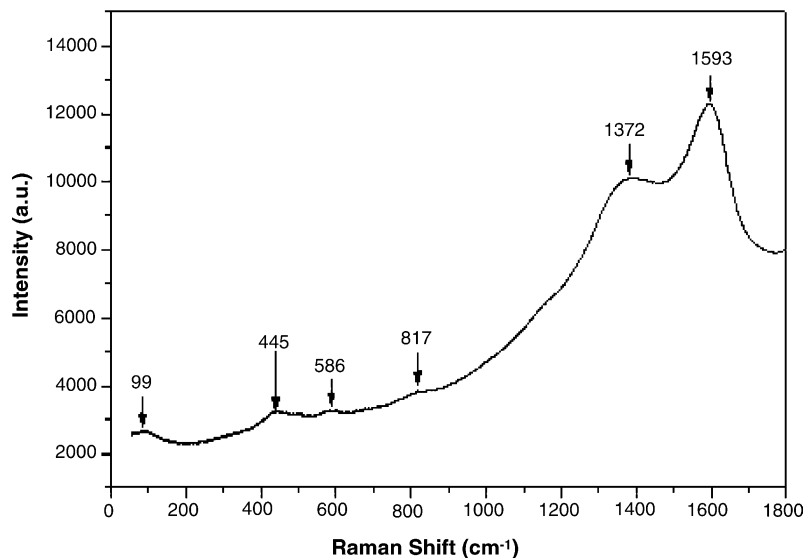


Fig. 2. Raman spectrum of ZnO matrix.

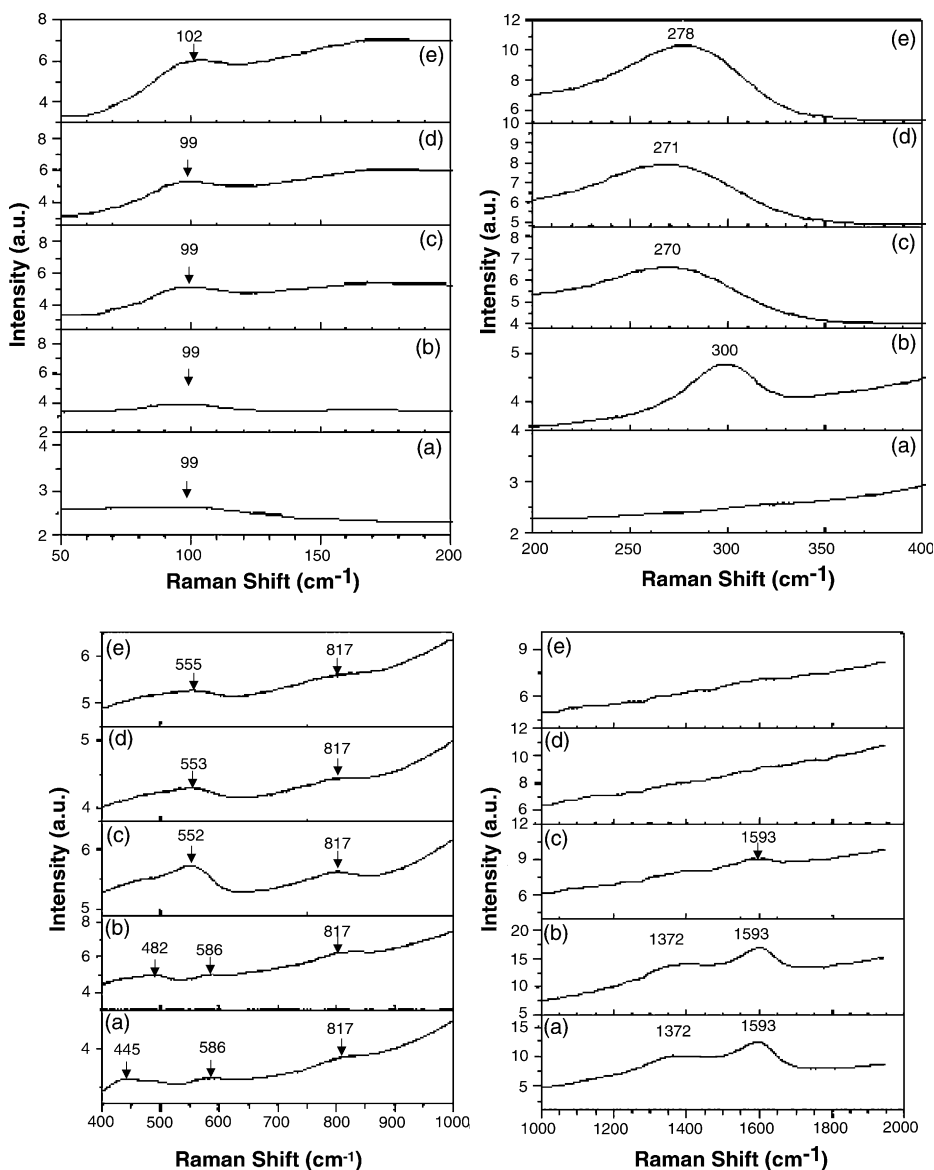


Fig. 3. Raman spectra in different spectral ranges for (a) ZnO matrix and Ge/ZnO nanocomposites, (b) as-deposited and annealed at (c) 200 °C, (d) 400 °C and (e) 600 °C.

tures are presented for different spectral ranges. The peak corresponding to the $E_2^{(1)}$ mode of ZnO is observed in the 50–200 cm^{-1} spectral range. The intensity of the $E_2^{(1)}$ mode increased on annealing. It should be attributed to the improvement of the crystal quality of the ZnO matrix. The peak shifts towards higher frequencies with the increase of annealing temperature.

In the 200–400 cm^{-1} spectral range, a new peak at about 300 cm^{-1} is revealed. We observed that the intensity and position of the peak depend strongly on the annealing temperature of the films. With the increase of the temperature until 400 °C the peak position moves gradually towards smaller energies, but when the temperature of annealing increases beyond 400 °C the peak moves towards higher

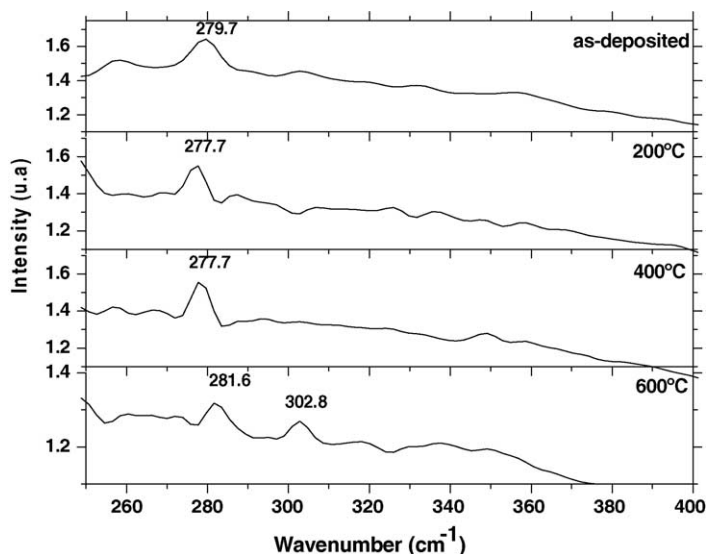


Fig. 4. The infrared absorption spectra of as-deposited and thermally annealed Ge/ZnO nanocomposite films.

energies. The peak has been assigned to the Ge–Ge TO (transverse optic) vibration [24] from Ge nanocrystallites in the ZnO matrix. The position of this peak is essentially the same as that observed for bulk Ge crystals [29,30] and that has been attributed to the $\Gamma_{25'}$ phonon at the center of the Brillouin zone [31]. The displacement of the peak towards smaller energies on annealing the samples up to 400 °C indicates the effect of phonon confinement in smaller nanocrystals. Whereas, the displacement of the peak towards higher energy on annealing the sample at 600 °C might be due to the crystallization of Ge. The intensity of the peak increased progressively on annealing. Among the other higher frequency emissions previously assigned to the nanosized ZnO particles, the intensity of the 586 and 817 cm^{-1} peaks gradually decreased in the composite films on increasing the annealing temperature; whereas, the peaks at around 1372 and 1593 cm^{-1} , disappeared upon annealing the composite films at 400 °C and above.

As the origin of those peaks in the Raman spectra was assigned to the nanosized ZnO particles in the films, such a variation of their intensity should reflect the variation of particles size in the composite films. To verify the effect, we recorded X-ray diffraction spectra of the composite films annealed at different temperatures (not shown here). The particle size of ZnO matrix was calculated from the prominent peaks

of the XRD patterns using Scherrer formula [32]. The calculated particle size of ZnO is given in Table 1. We can see that the particle size of ZnO increased from 9.0 to 17.0 nm on increasing the annealing temperature of the composite films up to 600 °C. Therefore, we believe that the reduction of the intensity or disappearance of the peaks (1372 and 1593 cm^{-1}) is due to an increase in particle size of ZnO matrix upon annealing.

IR absorption spectra of the Ge/ZnO nanocomposite films showed several peaks in the spectral range between 250 and 700 cm^{-1} . To make the analysis simpler, the whole IR spectra were divided into two regions; the first interval range from 250 to 400 cm^{-1} , and the second interval from 400 to 700 cm^{-1} . Fig. 4 shows the IR absorption spectra in the first region for the as-deposited and thermally annealed Ge/ZnO composite films. In the spectrum of as-deposited sample a peak appeared at about 280 cm^{-1} . On annealing at 200 or 400 °C, the position of the absorption peak shifted towards shorter wavenumber (277.7 cm^{-1}). However, with the increase of the annealing temperature to 600 °C, the peak position moved from 277.7 to 281.6 cm^{-1} . There appeared another peak at around 303 cm^{-1} for the sample annealed at 600 °C. We assigned the absorption peak at around 280 cm^{-1} to the deformation vibration of the Ge–O bond. A shift of this peak position is due to the

change of oxygen content in germanium oxide. The origin of the latter absorption peak is not very clear at the moment. However, it might be arising from the crystalline nc-Ge.

Fig. 5 shows IR spectra for ZnO matrix and Ge/ZnO composite films in the spectral range between 400 and 700 cm^{-1} . In this spectral range, the spectrum of the matrix exhibit three bands located at around 445, 535 and 615 cm^{-1} . The absorption bands at around 445 and 615 cm^{-1} were assigned to the E_2 mode (reported by Exarhos and Sharma [26] as Raman active) and $E_1(\text{LO})$ mode of ZnO, respectively. The band at around 535 cm^{-1} corresponds to the quartz substrate. In the absorption spectra of the as-deposited Ge/ZnO composite films the bands corresponding to the E_2 and $E_1(\text{LO})$ modes of ZnO are localized at around 439 and 591 cm^{-1} , respectively. With the increase of the annealing temperature, the position of these peaks did not change; however, for the film annealed at 600 $^\circ\text{C}$ we observed a peak at about 519 cm^{-1} . We assigned the peak to the symmetrical stretching vibration mode of Ge–O–Ge in germanium oxide. The position of the peak agrees well with the value reported by Mayerhöfer and Dunken [33] for their Ge nanocrystals embedded in silica matrix.

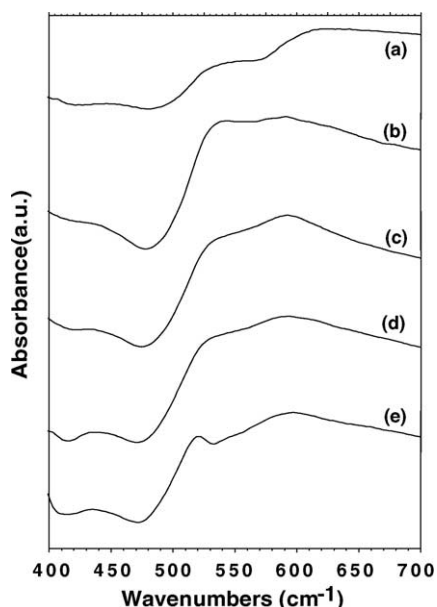


Fig. 5. The infrared absorption spectra of (a) ZnO matrix and Ge/ZnO nanocomposites films, (b) as-deposited and annealed at (c) 200 $^\circ\text{C}$, (d) 400 $^\circ\text{C}$ and (e) 600 $^\circ\text{C}$.

4. Conclusions

Ge nanocrystals embedded in ZnO matrix have been prepared by alternate rf sputtering technique. The size of the nc-Ge varied from 5.0 to 2.3 nm depending on the temperature of annealing. Apart from the $E_2^{(1)}$, $E_1(\text{LO})$ and $E_2^{(2)}$ vibrational modes characteristic of wurtzite ZnO, there appeared other IR bands at about 817, 1372 and 1593 cm^{-1} , which are supposed to be due to the nanometer sized crystallites of the matrix in the films. The 300 cm^{-1} peak, characteristic of Ge–Ge LO vibrational mode shifted towards lower frequency on annealing the films up to 400 $^\circ\text{C}$ due to phonon confinement in the smaller Ge nanocrystals. Appearance of absorption peaks at about 280 (Ge–O deformation vibration) and 519 cm^{-1} (SS mode of Ge–O–Ge) in the IR spectra of the composite films indicate the formation of oxide cap-layer at the surface of Ge nanocrystals. Reduction of intensity of both the absorption bands and increase of the Ge–Ge vibrational band in the Raman spectra upon annealing indicates the reduction of the oxide layer thickness upon annealing.

Acknowledgements

The work is partially supported by VIEP-CON-ACyT-SEP (grant no. II1302), Mexico. The authors thank G. Casarrubias Segura for his help in preparing the samples.

References

- [1] J.H. Sinfelt, G.D. Meitzner, *Accounts Chem. Res.* 26 (1993) 1.
- [2] Y. Wang, *Accounts Chem. Res.* 24 (1991) 133.
- [3] L. Brus, *IEEE J. Quant. Electron.* QE-22 (1986) 1909.
- [4] L. Brus, *Appl. Phys. A* 53 (1991) 465.
- [5] S. Takeoka, *Phys. Rev. B* 58 (1998) 12.
- [6] Y.X. Jie, Y.N. Xiong, A.T.S. Wee, C.H.A. Huan, W. Ji, *Appl. Phys. Lett.* 77 (2000) 3926.
- [7] L.T. Canham, *Appl. Phys. Lett.* 57 (1990) 1046.
- [8] A.G. Cullis, L.T. Canham, *Nature* 353 (1991) 335.
- [9] Y. Kanemitsu, H. Uto, Y. Masumoto, T. Maeda, *Appl. Phys. Lett.* 61 (1992) 2187.
- [10] L.E. Brus, P.F. Szajowski, W.L. Wilson, T.D. Harris, S. Schuppler, P.H. Citrin, *J. Am. Chem. Soc.* 117 (1995) 2915.
- [11] U. Pal, G. Casarrubias Segura, O. Zarate Corona, *Sol. Energ. Mat. Sol. C.* 76 (2003) 305.

- [12] R. Hayashi, M. Yamamoto, K. Tsunetomo, Y. Osaka, H. Masu, *Jpn. J. Appl. Phys.* 29 (1990) 756.
- [13] Y. Maeda, *Phys. Rev. B* 51 (1995) 1658.
- [14] V. Ng, S.P. Ng, H.H. Thio, W.K. Choi, A.T.S. Wee, Y.X. Jie, *Mater. Sci. Eng. A* 286 (2000) 161.
- [15] S. Okamoto, Y. Kanemitsu, *Phys. Rev. B* 54 (1997) 1621.
- [16] B.R. Taylor, S.M. Kauzlarich, H.W.H. Lee, G.R. Delgado, *Chem. Mater.* 10 (1998) 22.
- [17] K.S. Min, K.V. Shcheglov, C.M. Yang, H.A. Atwater, M.L. Brongersma, A. POLman, *Appl. Phys. Lett.* 68 (1996) 2511.
- [18] M. Zacharias, J. Christen, J. Basing, D. Bimberg, *J. Non-Cryst. Solids* 198 (1996) 115.
- [19] M. Fujii, S. Hayashi, K. Yamamoto, *Appl. Phys. Lett.* 57 (1990) 2692.
- [20] Y.X. Jie, A.T.S. Wee, C.H.A. Huan, W.X. Sun, Z.X. Shen, S.J. Chua, *Mater. Sci. Eng. B* 107 (2004) 8.
- [21] D.C. Panie, C. Caragianis, T.Y. Kim, Y. Shigesato, *Appl. Phys. Lett.* 62 (1993) 2842.
- [22] Y. Maeda, *Phys. Rev. B* 51 (1995) 1658.
- [23] X.L. Wu, T. Gao, X.M. Bao, F. Yan, S.S. Jiang, D. Feng, *J. Appl. Phys.* 82 (1997) 2704.
- [24] H. Yang, R. Yang, X. Wan, W. Wan, *J. Cryst. Growth* 261 (2004) 549.
- [25] N. Ashkenov, B.N. Mbenkum, C. Bundesmann, V. Iede, M. Lorenz, D. Spemann, E.M. Kaidashev, A. Kasic, M. Schubert, M. Grundmann, *J. Appl. Phys.* 93 (2003) 126.
- [26] G.J. Exarhos, S.K. Sharma, *Thin Solid Films* 270 (1995) 27.
- [27] Y.F. Lu, H.Q. Ni, Z.H. Mai, Z.M. Ren, *J. Appl. Phys.* 88 (2000) 498.
- [28] H. Zhou, H. Alves, D.M. Hoffmann, W. Kriegseis, B.K. Meyer, G. Kaczmarczyk, A. Hoffmann, *Appl. Phys. Lett.* 88 (2002) 210.
- [29] M.H. Ludwig, R.E. Hummel, S.S. Chang, *J. Vac. Sci. Technol. B* 12 (1994) 3023.
- [30] X.L. Wu, T. Gao, X.M. Bao, F. Yan, S.S. Jiang, D. Feng, *J. Appl. Phys.* 82 (1997) 2704.
- [31] M. Fujii, S. Hayashi, K. Yamamoto, *Appl. Phys. Lett.* 57 (1990) 2692.
- [32] B.D. Cullity, *Elements of X-ray Diffraction*, 2nd ed., Addison Wesley, 1978, pp. 99–102.
- [33] Th.G. Mayerhöfer, H.H. Dunken, *Vib. Spectrosc.* 25 (2001) 185.